Geodesy and Geodynamics 14 (2023) 26–34

Contents lists available at ScienceDirect

Geodesy and Geodynamics

journal homepage: http://www.keaipublishing.com/geog

Combination of Tsoft and ET34-ANA-V80 software for the preprocessing and analysis of tide gauge data in French Polynesia

Bernard Ducarme [a, *], Jean-Pierre Barriot [b], Fangzhao Zhang [c]

[a] Catholic University of Louvain, Georges Lemaître Centre for Earth and Climate Research (ELI), 1348 Louvain-la-Neuve, Belgium
[b] Geodesy Observatory of Tahiti, University of French Polynesia (UPF), Punaauia, French Polynesia
[c] College of Geodesy and Geomatics, Shandong University of Science and Technology, Qingdao 266590, China

ARTICLE INFO

Article history:
Received 15 November 2021
Accepted 6 May 2022
Available online 15 June 2022

Keywords:
Tide gauges
Tidal data processing
Mean sea level

ABSTRACT

Since 2008 a network of five sea-level monitoring stations was progressively installed in French Polynesia. The stations are autonomous and data, collected at a sampling rate of 1 or 2 min, are not only recorded locally, but also transferred in real time by a radio-link to the NOAA through the GOES satellite. The new ET34-ANA-V80 version of ETERNA, initially developed for Earth Tides analysis, is now able to analyze ocean tides records. Through a two-step validation scheme, we took advantage of the flexibility of this new version, operated in conjunction with the preprocessing facilities of the Tsoft software, to recover corrected data series able to model sea-level variations after elimination of the ocean tides signal. We performed the tidal analysis of the tide gauge data with the highest possible selectivity (optimal wave grouping) and a maximum of additional terms (shallow water constituents). Our goal was to provide corrected data series and modelled ocean tides signal to compute tide-free sea-level variations as well as tidal prediction models with centimeter precision. We also present in this study the characteristics of the ocean tides in French Polynesia and preliminary results concerning the non-tidal variations of the sea level concerning the tide gauge setting.

1. Introduction

This study presents the results of the preprocessing and analysis of the sea level monitoring of the five stations established since 2007 by the Geodesy Observatory of Tahiti (OGT), University of French Polynesia (UPF) in the French Polynesia part of the South Pacific area (Fig. 1), and maintained by the hydrographic and oceanographic survey branch of the French Naval Hydrographic and Oceanographic Service (SHOM): Vairao (Tahiti-Iti), Mangareva/Rikitea (Gambier Archipelago), Tubuai (Austral Archipelago), Makemo and Rangiroa (Tuamotu Archipelago). As all these five stations include GPS monitoring, they can be considered geodetic tide gauges focusing on the monitoring of the mean sea level. Other tide gauges exist, maintained by the University of Hawaii (UH) and the French Atomic Energy Commission (CEA). However, they mainly focus on the monitoring of tsunamis, the only exception being the UH tide gauge of the Papeete harbor, also equipped with a GPS receiver. We used also for comparison purposes the tide Gauges of the University of Hawaii at Mangareva (RikiteaUH).

Our goal was to provide corrected data series and modelled ocean tides signal to compute tide free sea-level variations. Two data collection packages, titled "SEA LEVEL collected from TIDE STATIONS in South Pacific Ocean from 2009 to 06–13 to 2021-01-28 (ref. 0244182)", have been accepted by the NOAA National Centers for Environmental Information (NCEI) [1]. The first one is relative to the original sampling rate, and the second one is relative to the hourly averaged data, both under NCEI accession number 0244182.

Ocean tide modelling and prediction have always been important for the safety of seafarers, but the determination of the mean sea level (MSL) and its variations, due to climate changes, is now a

* Corresponding author.
E-mail addresses: bf.ducarme@gmail.com (B. Ducarme), jean-pierre.barriot@upf.pf (J.-P. Barriot), fzzhang@sdust.edu.cn (F. Zhang).

Peer review under responsibility of Institute of Seismology, China Earthquake Administration.

Production and Hosting by Elsevier on behalf of KeAi

https://doi.org/10.1016/j.geog.2022.05.002

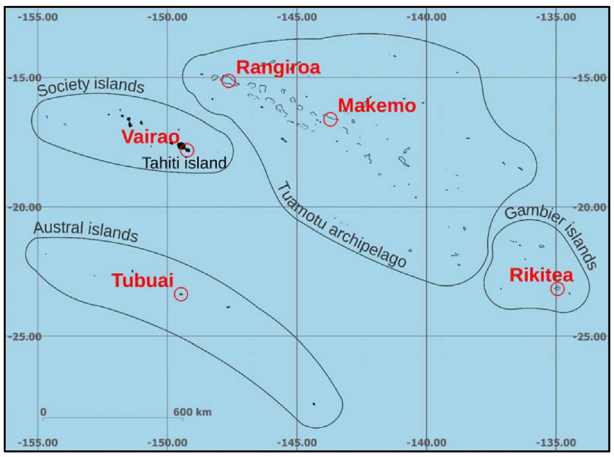

Fig. 1. The network of Geodetic Tide Gauges in French Polynesia (red points). Tahiti is the capital island of French Polynesia, with 2/3 of the total population.

hotspot of oceanographic research [2]. In French Polynesia, the situation is complex, with inter-annual modulations on one side and vertical subduction of many volcanic edifices [3,4]. The early detection of tsunami waves is a high priority for protecting human populations in coastal areas.

We present here, first, our methodology of sea-level modelling, and how to process and analyze noisy and gappy data with a low signal-to-noise ratio. In a second step, the tidal analysis results are used to illustrate the principal characteristics of the ocean tides signal in this area of the Pacific Ocean, as well as local distortions of the tidal signal in the lagoons. The tidal models derived from this analysis allow the tides prediction with a centimeter precision at different stations. Finally, we present preliminary non-tidal variations ΔRSL of the relative sea level (RSL), measured with respect to the tide gauge setting. As the GPS observations are not yet processed, our results are not directly comparable with variations of the mean sea level (ΔMSL), as we have

$$\Delta\mathrm{MSL} = \Delta\mathrm{RSL} + \Delta h$$

where Δh represents the vertical ground displacement that should be derived from GPS observations [5].

2. Data preprocessing and validation

All the five tide gauges operated in French Polynesia by OGT obey the guidelines set up by SHOM [6]. They are equipped with: GNSS antenna and receiver, radar and pressure gauge sensors for sea-level monitoring, and a satellite GOES (Geostationary Operational Environmental Satellite) radio transmitter. We use the RADAR seal level sensor QHR104 of Vaisala (Fig. 2). Measurement is done in pulses, the so-called pulse procedure, where a transmitter sends out a short microwave pulse, followed by a period when the receiver picks up the signals reflected by the water. The accuracy is better than 5 mm. At RikiteaUH an encoder has been installed on an old tide gauge with float sensor in parallel with the RADAR and the pressure gauge. The sea level sampling corresponds to measurements taken every second and averaged over 1 min. All the data are stored locally and transferred to the UPF database when maintenance takes place. They are also transferred via satellite at least every 2 min by a UHF radio-link to the NOAA (National Oceanic and Atmospheric Administration of the USA) through the GOES satellite constellation, but without neither GPS *in situ* time-tagging nor GPS positioning data, to save transmission bandwidth. They are *ex-situ* time-tagged again upon arrival at the NOAA and stored at the Sea Level Station Monitoring Facility site [7] (VLIZ/IOC). Additional information about the stations and the data are available in Refs. [8,9].

Fig. 2. The typical Tide Gauge geodetic station of Vairao (Tahitilti peninsula of Tahiti). One can see the RADAR altimeter (vertical cornet on the right side), the GOES UHF Yagi antenna on the roof as well as the GPS radome and a solar panel.

Sometimes the local recording at the tide gauges was not operating, so the only source of data was the VLIZ/IOC database, sometimes, the GOES data link was not operating, so the only source of data was the local records on the tide gauges.

We first did a cross-comparison of the VLIZ/IOC data sets versus the UPF data set based on the coherence of the tidal phases after preliminary analysis. We found that the time re-tagging by VLIZ/IOC was often off by several minutes with respect to the GPS time tagging done at the tide gauges, and sometimes shifts up to 1 h were found. We, therefore, elected to retain the UPF data sets whenever possible. When the UPF and VLIZ/IOC time series have no overlapping, it was always possible to correct any timing error by considering the coherence of the phase of the main tidal waves, as explained in section 2. The observation time corresponds to the middle of the time interval, i.e. it is shifted of 30 s for a 1-min integration period. This time shift is negligible for long period phenomena which are the main goal of the sea level measurements in French Polynesia. For tidal analysis, a time shift of 30 s can be introduced during the analysis procedure.

We routinely preprocessed and analyzed the RADAR and pressure gauge data of the 6 stations. The preprocessing data flow, divided into 3 levels, is shown in Fig. 3.

LEVEL 1 data are obtained by rewriting the original records (locally stored UPF or radio transferred VLIZ/IOC data) in the so-called PRETERNA format. It is impossible to directly use these raw data to compute a final data set with an hourly sampling rate due to several remaining errors, either incorrect data producing spikes, jumps, and gaps or timing problems.

During the first step, between LEVEL 1 and LEVEL 2, the data sequence is checked, and preliminary tidal analyses are performed with the software ET34-ANA-V80 designed by K. Schueller [12–14], in order to prepare a preliminary tidal model and detect timing errors. It is always possible to detect any timing error by considering the coherence of the phase of the main tidal waves, with the phase computed from the UPF data archived with the correct *in situ* timing. In the semi-diurnal band, a timing error of 2 min produces a phase difference of one degree at the frequency of 2 cycles-per-day (cpd). If necessary, a time shift is applied. The outliers, mainly unwanted “spikes”, are identified and removed using the software Tsoft [9,15] and a “remove-restore” procedure. The preliminary tidal model is subtracted from the raw data, the corrections are applied on the residues and the corrected tidal signal is reconstructed, summing up the removed tidal model again. Finally, the small interruptions (gaps) are tagged and interpolated with the same procedure (Fig. 4).

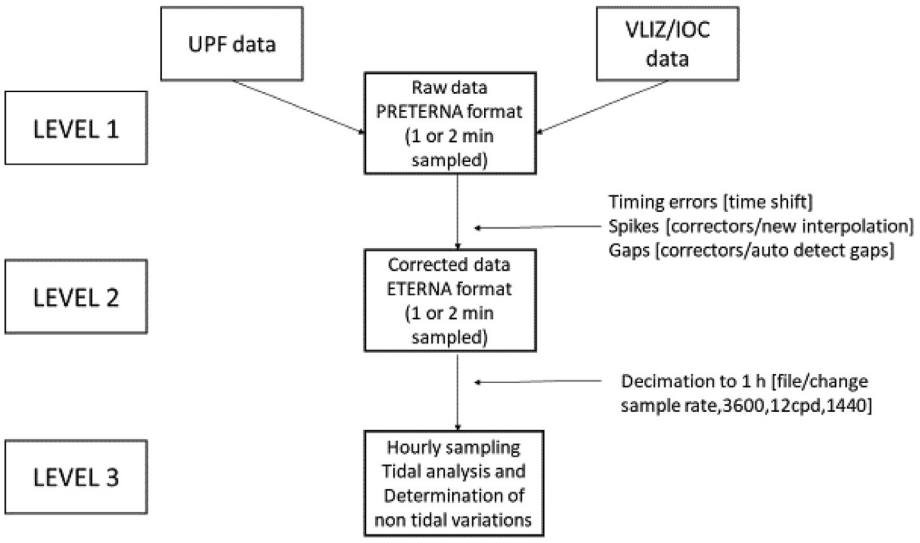

Fig. 3. Data flow during preprocessing. The corrective actions listed in the square brackets are performed with the TSoft software [10]. The PRETERNA and ETERNA formats are described in [11].

The float sensor at Rikitea UH presented several jumps after short interruptions. It was impossible to correct them accurately with the Tsoft option "auto correct steps", as gaps are associated with the jumps. The option "correctors/new step" is only a manual adjustment, and thus not so accurate. A better solution was to introduce in the tidal analysis auxiliary channels including a unit step function corresponding to each jump (Fig. 5). These auxiliary unknowns are adjusted during the LSQ analysis procedure. The values of the jumps are computed with millimeter precision.

In the second step of data validation, between LEVEL 2 and LEVEL 3, the sampling rate of the data is reduced to 1 h by means of a standard filter provided by TSoft. This least-squares filter has a cutoff frequency at 12cpd and a half length of one day i.e. 1440 or 720 samples for a 1 min or 2 min original sampling rate. This reduction presents the advantage of filtering out the higher

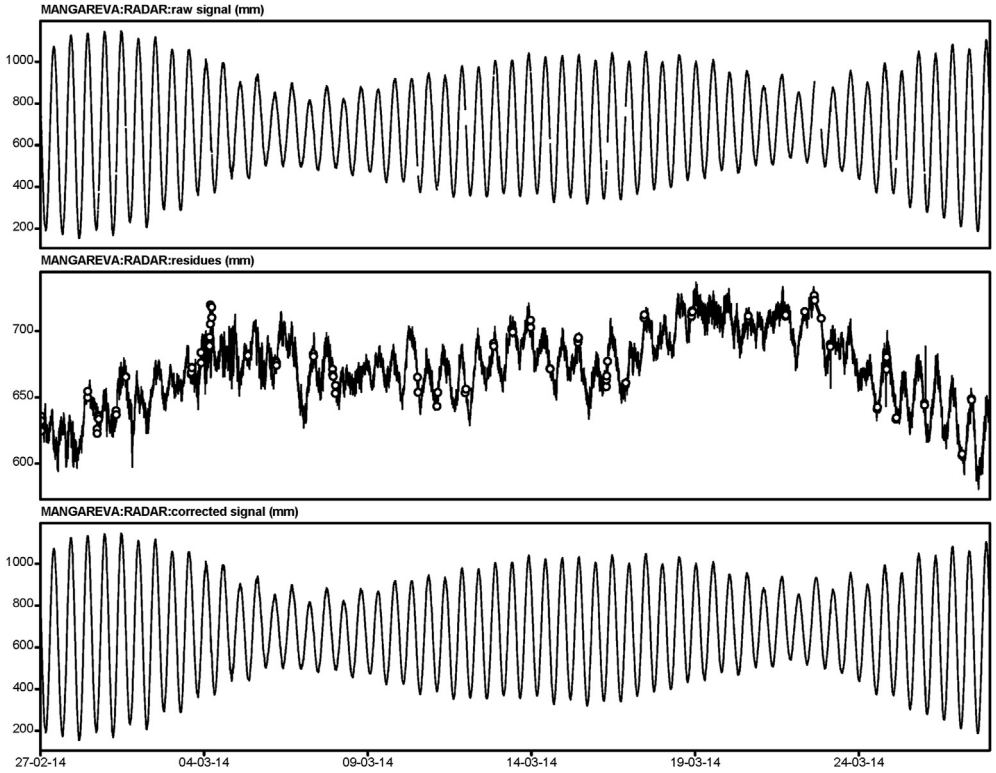

Fig. 4. Example of remove-restore procedure for automatic correction of gaps for the RADAR signal at Rangiroa. Top: raw signal (mm) with numerous gaps; Middle: residues (mm) after subtraction of the theoretical tides from the raw signal (remove step). Gaps detected by the "auto detect gaps" corrector indicated by white dots are linearly interpolated; Bottom: corrected signal (mm) obtained by the addition of the theoretical tides to the corrected residues (restore step).

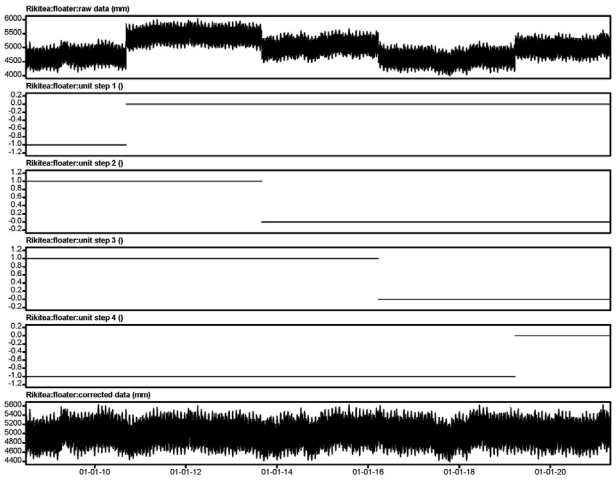

Fig. 5. Automatic jump correction for the float sensor with encoder at RikiteaUH. From top to bottom: raw signal (mm); the 4 unit-step functions introduced as auxiliary channels; corrected series (mm).

frequency noise present in the original data, while keeping the tidal signal up to 12cpd. This third-level database is convenient for most applications, except detection of transient signals such as tsunamis or swells. Tidal analyses are performed to compute and subtract the ocean tides signal. The computed residues are a preliminary representation of the variations of the Mean Sea Level due, in the first order, to meteorological phenomena and in the second-order to climate-related effects.

3. Tidal analysis procedure

Validated and preprocessed data have been analyzed with the ETERNA system software [16]. The latest version of the software ET34-ANAL-V80 [12] proposes a special option for ocean tides analysis and prediction in agreement with oceanographic conventions (i.e. phases refer to Greenwich and phase lags are counted positive). Moreover, the changes of signs of the tidal potential with latitude are not taken into account by oceanographers. The program can be downloaded from http://ggp.bkg.bund.de/eterna/.

Two useful new features have been implemented in ET34-ANA-V80:

- An automatic detection of spectral peaks not included in the tidal analysis model.
- The computation of the correlation between the different unknowns.

The program performs a spectral analysis of the tidal residues and proposes a list of the peaks exceeding a given threshold level. These additional harmonics, not included in the tidal potential, are generally non-linear terms from the oceanic or meteorological origin, such as shallow water components or seasonal modulations of the pressure waves S_m, $m > 2$. An exhaustive list of these terms is provided in the software.

The program computes the correlation between all the unknowns included in the tidal analysis procedure. A “global RMSE error amplifier”, which is the ratio between the RMSE propagated with and without including correlations, summarizes the effect of the existing correlations. This coefficient equals one if the corresponding parameter is independent of all the others. If the value increases, it is necessary to check the correlation table to identify the source of the problem and reduce the number of groups or suppress the corresponding additional harmonics.

We performed the tidal analysis of the tide gauge data with the highest possible selectivity (optimal wave grouping) and a maximum of additional harmonics on the basis of the new features described above.

4. Ocean tides results

A detailed comparison of the pressure gauge and RADAR data can be found in Ref. [9]. Pressure data do not have a sufficiently long-term stability to be useful for the MSL determination. However, they can replace missing RADAR records or confirm them for the detection of special events such as tsunami occurrences. They agree with RADAR data regarding what concerns the ocean tides [9]. In Tables 1 and 2, the conclusions of RADAR data analysis using the global data set (UPF + VLIZ/IOC) at each station.

The results of Tables 1 and 2 will be used to compute accurate tidal predictions. It is difficult to determine their accuracy. It will depend on the accuracy of the calibration of the RADAR on one side, and on the signal to noise ratio in the tidal records on the other.

Concerning the calibration, the Mangareva/Rikitea station is very helpful. The comparison of MangarevaUPF and RikiteaUH is a test of the precision of the calibration of the RADAR altimeter, as the two stations are separated by less than 1 km. The amplitudes of the tidal waves agree at the millimetric level (Table 2). A linear regression between the two instruments gives:

$$\mathbf{RADAR}_{\mathrm{UH}} = 1.0025 \pm 0.0002 \times \mathbf{RADAR}_{\mathrm{UPF}}\ r = 0.999$$

The calibrations of the two instruments are thus in agreement within 0.25%. It ensures a precision of 2 mm for a peak tidal amplitude of 80 cm. The slight phase difference in phase is due to the fact that the UH station is located in a fishpond, totally buffered from the lagoon, while the UPF station is located in the harbor.

We can evaluate indirectly the precision of the tidal prediction looking at the amplitude of the tidal residues after the least-squares analysis. The residual signal is concentrated in the semi-diurnal band. We compare the M2 amplitude in the spectrum of the residual signal to its value in the spectrum of the original signal. We can extrapolate this attenuation of the signal at M2 frequency to the attenuation of the global tidal signal and thus deduce the amplitude of the residual tidal signal. We get the following peak to peak amplitudes: Rangiroa 12 mm, Makemo 20 mm, Vairao 23 mm, Tubuai 18 mm, Mangareva 10 mm and Rikitea 6 mm. It is reasonable to state that the precision of the tidal prediction is close to ±1 cm in Makemo, Tubuai and Vairao on one side and close to±0.5 cm in Rangiroa and Mangareva/Rikitea.

The tidal regime is described by the tidal form factor *F*, initially introduced by van der Stok [17] under the form.

$$F = \frac{K1 + O1}{M2 + S2}$$

It expresses the ratio between the main diurnal (D) and semi-diurnal (SD) waves.

There are three regime types:

$F > 3$ Diurnal: 1 High, 1 Low per day.

$0.25 < F < 3$: Mixed 2 Highs, 2 Lows per day, but of different strength.

$F < 0.25$: Semidiurnal 2 Highs, 2 Lows per day, similar strength.

A fourth type was introduced by Courtier [18], who split the mixed-mode into mixed semidiurnal–dominant and mixed diurnal-dominant.

Table 1
Tidal amplitudes A and Greenwich phases α (RADAR, hourly sampling).

Wave	Rangiroa 14°56,75′S 147°42,36′W 2009/06–2021/02 3644 days Goodness of fit R^2 98.3% $m0 = 54$ mm $F = 0.13$		Makemo 16°37,63′S 143°34,15′W 2013/10–2021/01 2602 days Goodness of fit R^2 97.7% $m0 = 103$ mm $F = 0.11$		Vairao 17°48,35′S 149°17,7′W 2011/07–2021/01 3197 days Goodness of fit R^2 99.1% $m0 = 51$ mm $F = 0.15$	
	A(mm)	α(°)	A(mm)	α(°)	A(mm)	α(°)
O1	6.3 ± 0.2	173.8 ± 1.4	11.7 ± 0.3	178.4 ± 1.7	15.6 ± 0.3	87.9 ± 1.1
K1	13.5 ± 0.2	−99.9 ± 0.6	13.1 ± 0.3	−69.6 ± 1.4	11.9 ± 0.3	64.3 ± 1.3
ALF2	5.7 ± 0.3	11.5 ± 3.1	1.4 ± 0.3	−29.8 ± 13.3	5.5 ± 0.5	35.2 ± 5.4
M2	116.2 ± 0.3	39.7 ± 0.2	171.9 ± 0.3	73.0 ± 0.1	100.8 ± 0.5	−54.0 ± 0.3
BET2	4.0 ± 0.3	−170.2 ± 4.4	0.8 ± 0.3	−137.4 ± 22.2	4.7 ± 0.5	31.2 ± 6.4
S2	36.0 ± 0.3	13.3 ± 0.5	45.7 ± 0.3	45.2 ± 0.4	85.2 ± 0.5	−40.5 ± 0.4
M3	1.9 ± 0.1	−62.5 ± 3.4	2.1 ± 0.1	−37.6 ± 2.5	2.7 ± 0.1	−77.0 ± 2.6
M4	17.3 ± 0.2	−163.9 ± 0.6	16.7 ± 0.2	57.1 ± 0.5	0.9 ± 0.2	170.0 ± 9.7
3MK2	1.7 ± 0.4	117.0 ± 11.4	2.4 ± 0.4	161.4 ± 8.9	1.3 ± 0.5	148.3 ± 22.5
3MO2	2.0 ± 0.4	152.0 ± 10.7	2.2 ± 0.4	178.4 ± 9.8	2.8 ± 0.5	146.5 ± 9.7
Sa	20.3 ± 2.0	119.5 ± 5.2	65.9 ± 5.2	122.6 ± 3.5	22.5 ± 1.7	82.7 ± 3.7
Ssa	15.8 ± 2.0	8.8 ± 6.9	23.8 ± 4.0	42.1 ± 9.5	11.8 ± 1.7	2.2 ± 8.3
Sta	4.8 ± 2.0	207.3 ± 22.0	11.8 ± 8.0	−16.9 ± 19.0	3.5 ± 1.7	86.5 ± 28.1

m0: RMS error on one observation (unfiltered data).

Table 2
Tidal amplitudes A and Greenwich phases α (RADAR, hourly sampling).

Wave	Tubuai 23°20,50′S 149°28,53′W 2010/02–2021/01 3177 days Goodness of fit R^2 98.9% $m0 = 74$ mm $F = 0.17$		Mangareva 23°07,07′S 134°58,13′W 2012/05–2021/01 2358 days Goodness of fit R^2 99.3% $m0 = 59$ mm $F = 0.12$		RikiteaUH 23°07,33′S 134°58′W 200806/202104 4679 days Goodness of fit R^2 99.9% $m0 = 61$ mm $F = 0.12$	
	A(mm)	α(°)	A(mm)	α(°)	A(mm)	α(°)
O1	21.6 ± 0.2	65.9 ± 0.5	17.8 ± 0.2	47.5 ± 0.7	18.1 ± 0.1	46.7 ± 0.4
K1	21.2 ± 0.2	50.0 ± 0.5	23.9 ± 0.2	6.6 ± 0.5	23.7 ± 0.1	6.4 ± 0.3
ALF2	1.7 ± 0.3	−71.9 ± 9.4	2.3 ± 0.2	122.5 ± 5.6	1.5 ± 0.1	106.8 ± 5.4
M2	153.6 ± 0.3	−101.8 ± 0.1	264.0 ± 0.2	−8.5 ± 0.1	264.0 ± 0.1	−10.1 ± 0.0
BET2	2.6 ± 0.3	−37.1 ± 6.1	1.7 ± 0.2	−95.0 ± 7.4	1.8 ± 0.1	−95.2 ± 4.4
S2	103.8 ± 0.3	−51.7 ± 0.2	92.1 ± 0.2	−50.3 ± 0.2	92.3 ± 0.1	−51.8 ± 0.3
M3	2.4 ± 0.1	−73.0 ± 1.8	5.3 ± 0.1	−127.3 ± 0.7	5.3 ± 0.1	−130.2 ± 0.5
M4	1.8 ± 0.1	−164.1 ± 0.6	1.0 ± 0.1	−172.2 ± 2.6	1.4 ± 0.1	−173.3 ± 1.5
3MK2	2.4 ± 0.3	151.0 ± 7.1	3.9 ± 0.2	99.1 ± 3.7	3.4 ± 0.1	109.7 ± 2.5
3MO2	1.8 ± 0.3	171.9 ± 9.8	4.3 ± 0.2	114.3 ± 3.3	4.5 ± 0.1	112.7 ± 2.0
Sa	26.5 ± 3.0	62.4 ± 6.1	27.5 ± 2.8	118.6 ± 5.5	36.5 ± 1.8	98.3 ± 2.8
Ssa	10.9 ± 3.0	−36.8 ± 15.4	6.1 ± 2.8	−43.5 ± 26.4	4.0 ± 1.8	−73.4 ± 26.0
Sta	14.0 ± 3.0	139.3 ± 12.0	12.4 ± 2.8	96.9 ± 12.9	9.5 ± 1.8	127.3 ± 11.1

m0: RMS error on one observation (unfiltered data).

In French Polynesia, the tidal regime is always pure semidiurnal with a form ratio lower than 0.2 (Tables 1 and 2).

It is possible to get an idea of the tidal amplitudes in the open ocean near the stations from high-resolution ocean tides models such as FES04 [19]. With a grid of 0.125° × 0.125°, it has a resolution close to 14 km. The tidal amplitudes are generally lower in the stations located to the West, with M2 amplitudes increasing from 17 cm to 27 cm from East to West. The Vairao station is exceptional with an M2 amplitude of 10 cm, similar to the S2 one (8 cm). The results of Tables 1 and 2 are coherent with the FES04 model at Vairao, Tubuai and Mangareva for M2 and S2 (Fig. 6a and b). However, in Rangiroa and Makemo, the observed semi-diurnal tidal amplitudes are 40% lower than expected, and the phases increase of 17° in Rangiroa, and 67° in Makemo. It means that the observed tide presents a lag of 30 min, and more than 2 h with respect to the open sea, respectively. This attenuation and deformation of the tidal pattern is associated with a strong non-linearity expressed by the large amplitude of the M4 component, up to 17 mm in place of only 1 mm in the other stations. M6 also increases to a value of 5 mm. One can see here the influence of the lagoons.

The annual modulation waves of M2 (ALFA2, BETA2) are generally amplified. In the tidal potential, the ratio between the annual modulations and the principal component M2 is lower than 0.004, but in Rangiroa and Vairao these waves reach an amplitude of 5 mm, i. e. 5% of M2 amplitude. As a result, there is a 10% change of the apparent amplitude of M2 with a minimum at the end of the civil year. This modulation is illustrated in Fig. 7. The observed tidal signal is compared with a tidal prediction without the annual modulation of M2. The apparent sensitivity is the coefficient of proportionality.

The annual component Sa is obviously associated with the weather pattern with a minimum in January (austral summer). Its amplitude is close to 30 mm, except in Makemo where it reaches 60 mm. The noise level also displays a clear annual pattern with a maximum during austral winter.

In the semi-diurnal band, it was possible to extract the tiny waves 3MK2 and 3MO2 generated by the third-degree tidal

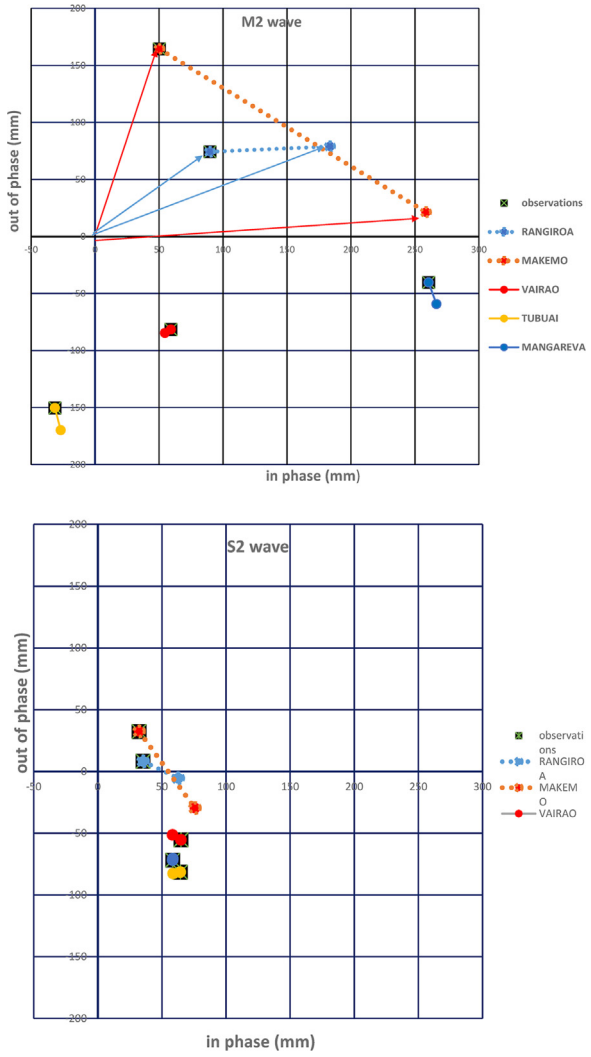

Fig. 6. A: Tidal wave M2 components computed from observation (inserted in black squares) and FES04 ocean tides model. For Rangiroa and Makemo, the tidal vectors are displayed, showing the amplitude reduction and phase advance of the observations with respect to the FES04 model (Rangiroa 17°, Makemo 67°). B: Tidal wave S2 components computed from observation (inserted in black squares) and FES04 ocean tides model.

potential. The amplitude is only a few millimeters, but the phase of the two waves are coherent in each station within the associated RMS errors (Tables 1 and 2). It confirms the results obtained in this area using satellite altimetry [20]. The phase is close to 150° in the 3 western stations Rangiroa, Vairao and Tubuai.

The 13-year long RADAR records. In RikiteaUH allowed the separation of the nodal waves for the main tidal components with a low correlation index. The results show that the nodal waves and the principal waves have the same amplification and the same phase difference, with respect to the equilibrium tides (Table 3). It means that the separation of the nodal waves is not required to get an accurate tidal prediction model.

In Table 4, we list higher degree tides and pressure waves with a signal-to-noise ratio close to 20 dB, which corresponds to a RMS error of 10% on the amplitude of the waves. Most of them have amplitudes lower than 1 mm. The meteorological waves *Sn* have been detected up to degree $n = 11$. S3 is surrounded by its annual modulation waves SP3 and SK3. The amplitude of the Sn waves is lower in Rangiroa. Higher degree tides M6 and M8 are present with a larger amplitude in Rangiroa. M10 is only found in Rangiroa. It is an illustration of the deformation of the tidal flux entering the lagoon. The main shallow water components detected in all stations is MS4 with an amplitude up to 10 mm in Rangiroa. The signal to noise ratio is worse in Makemo, where we can only detect a large MS4 (7.2 mm) and M8, confirming the distortion of the tidal signal.

5. Non tidal effects

The computed residues are a preliminary representation of the variations of the relative sea level (ΔRSL) measured with respect to the grounded tide gauge benchmark. They are produced, to the first order, by meteorological phenomena and, to the second order, by climate related effects. However, true variations of the MSL (ΔMSL) require the determination by Global Navigation Satellite Systems (GNSS) of the geocentric vertical land motion of the benchmark Δh [5]. We have the relation

$$\Delta\mathrm{MSL} = \Delta\mathrm{RSL} + \Delta h$$

In the atolls and volcanic islands of the French Polynesia, land subsidence is a well-known fact [4,21], and the results presented here will only consider ΔRSL.

The pressure gauge shows the same long-term fluctuations as the RADAR, with seasonal characteristics, but is affected by a steady drift and jumps. We can only consider the RADAR data for the determination of the relative sea level (RSL).

For dataset presenting jumps and long-term variations, it is helpful to apply the filter N1H1KSHW (Tsoft manual, p68), which eliminates at least 99% of the periodic signals with periods larger than one month. In our case, the tidal analysis provides a much lower RMS error on one observation using the filtered data than with the unfiltered data set, as shown in Table 5. It is due to large long-term fluctuations from meteorological origin on the sea level. It means that these long term fluctuations should be modelled, or at least averaged over a very long time span. The longest time span does not exceed 13 years and is thus too short to assess “secular trends”. Moreover, some station records present gaps, and the mean RSL values of the consecutive blocks can be different. It was only possible to determine tentatively long-term variations ΔRSL of the RSL (Table 5).

In Makemo and Mangareva, the long-term sea-level change is not statistically valid. Given the ΔRSL values and the corresponding time interval, the sea level seems to increase by 7.3 ± 0.3 mm/year In Rangiroa, 3.8 ± 0.3 mm/year in Vairao and 4.9 ± 0.5 mm/year in Tubuai. Due to the long period of nearly 13 years without interruption covered by the University of Hawaii tide gauges in Mangareva/Rikitea, the determination of a long-term trend is more reliable. The variation of the RSL between July, 2008 and April, 2021 is ΔRSL = +25.2 ± 2.3 mm, i.e. +2.0 ± 0.3 mm/year.

Sea level changes and vertical land motions have been reported in several publications for the stations Papeete (close to Vairao) and Rikitea [3,21]. In Table 6, we list the different values of ΔRSLy (annual relative sea level trend at the tide gauges and Δh (vertical motion rate from GPS observations) found in these papers. The vertical subduction rate is low, if you except the larger value at Papeete in Ref. [4]. The values of ΔRSLy confirms fully our results at Rikitea, while the apparent elevation rate of 4 mm/year in Vairao is compatible with the previous results at Papeete. A large elevation rate at Rangiroa was already reported. The early part (2009–2013) of Tubuai is certainly perturbed for some reasons, considering the results given in Table 6. In comparison, the trend in total sea level from 1993 to 2019 using observations from satellite altimeters is estimated at 2.75 ± 1.46 mm/year in Tahiti and 2.76 ± 1.18 mm/year in Rikitea [22].

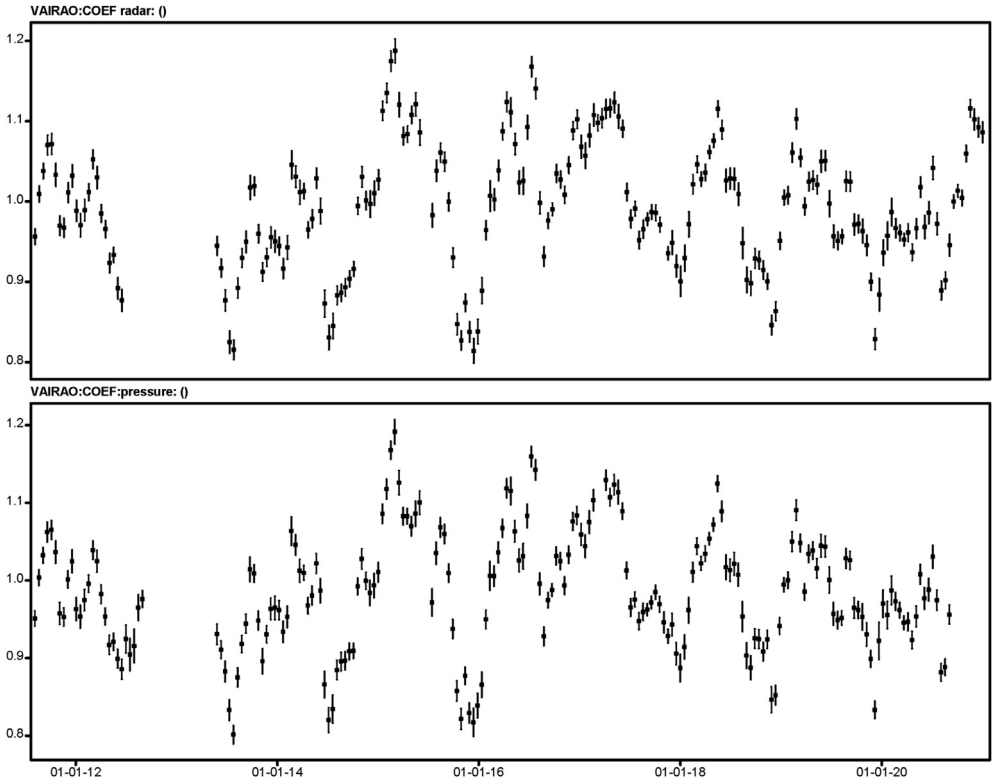

Fig. 7. A moving window adjustment of a simplified tidal model with no annual modulation of M2 on Vairao data (consecutive blocks of 30 days shifted by 15 days), showing the ratio between observations and model (upper RADAR, lower pressure). The agreement between two different sensors is a proof that these variations of the apparent sensitivity are real.

Table 3
Comparison of nodal waves with the corresponding principal wave.

wave	Angular speed (deg/h)	A_{th} (mm)	A_{obs} (mm)	A_{obs}/A_{th}	RMS error	Phase (°)	RMS error
•O1-	13.940829	13.7	3.5	0.256	0.010	43.7	2.1
O1	13.943036	72.8	18.8	0.248	0.002	46.5	0.4
K1	15.041069	102.4	23.8	0.233	0.001	6.2	0.4
•K1+	15.043275	13.9	3.4	0.243	0.010	4.6	2.5
•M2-	28.981898	7.7	10.1	1.312	0.019	−10.1	0.8
M2	28.984104	206.9	263.8	1.275	0.001	−10.1	0.0
K2	30.082137	26.2	28.0	1.069	0.006	−58.9	0.3
•K2+	30.084344	7.8	8.4	1.079	0.022	−62.4	1.2
•M3-	43.473950	0.14	0.31	2.238	0.357	9.1	17.9
M3	43.476156	2.49	5.31	2.130	0.040	0.5	1.1

• Nodal wave.
A_{th}: amplitude of the corresponding equilibrium tides (geoid tides).
A_{obs}: observed amplitude, Phase: phase difference with equilibrium tides.

Table 4
Shallow water components and pressure waves with a signal to noise ratio close to 20 dB. Pressure waves are identified by *.

wave	Rangiroa	Vairao	Tubuai	Rikitea
	A(mm)	A(mm)	A(mm)	A(mm)
SP3*	1.3	2.2	2.2	2.3
S3*	0.7	1.3	1.3	0.3
SK3*	1.6	2.6	2.6	2.3
MS4	10.0	0.9	2.6	0.5
S4*	0.3	0.6		0.3
M5	0.6			
S5*	0.3	0.6	0.5	0.1
2MN6	2.0	0.6	0.5	0.4
M6	4.6	0.9	0.3	0.2
2MS6	2.9	0.6	0.4	0.4
S6*		0.4	0.2	0.6
S7*		0.2	0.1	0.2
M8	1.3		0.2	
S9*		0.2		0.2
M10	1.0			
S11*		0.1		0.1

Table 5
Mean Tide gauge Level (RSL) and RSL variations (ΔRSL) with RADAR (hourly sampling).

Rangiroa 2009/06–2021/02 3644 days *m*0 = 54 mm *m*0f = 19 mm		Makemo 2013/10–2020/12 2565days *m*0 = 103 mm *m*0f = 24 mm		Vairao 2011/07–2021/01 3197 days *m*0 = 51 mm *m*0f = 22 mm		Tubuai 2010/02–2021/01 3195 days *m*0 = 74 mm *m*0f = 15 mm		Mangareva 2012/05–2021/01 2009 days *m*0 = 59 mm *m*0f = 12 mm		RikiteaUH 2008/06/2021/04 4679 days *m*0 = 61 mm *m*0f = 10 mm	
RSL (mm)	epoch	RSL (mm)	epoch	RSL (mm)	epoch	RSL (mm)	epoch	RSL (mm)	epoch	RSL (mm)	epoch
374.4 ± 1.6	2009–2014			503.1 ± 2.4	2011–2014	686.5 ± 2.6	2010–2014	644.2 ± 2.6	2012–2016		
426.9 ± 1.6	2014–2018			530.9 ± 1.4	2014–2020	725.1 ± 3.2	2015–2020	646.6 ± 2.7	2018–2020		
429.0 ± 2.4	2014–2021										
404.0 ± 1.2	**2009–2021**	**653.6 ± 2.8**	**2013–2020**	**518.0 ± 1.2**	**2011–2021**	**706.0 ± 2.1**	**2010–2021**	**645.2 ± 2.0**	**2012–2021**	**678.6 ± 1.3**	**2008–2020**
ΔRSL		ΔRSL		ΔRSL		ΔRSL		ΔRSL		ΔRSL	
+84 ± 3 mm		−8 ± 5 mm		**+36 ± 3 mm**		**+54 ± 5 mm**		+7 ± 5 mm		**+25 ± 2 mm**	

m0: RMS error on one observation (unfiltered data).
m0f: RMS error on one observation (high pass filter N1H1KSHW applied for rejection of long period phenomena, Tsoft manual, p.68).

Table 6
Previous results found in the literature.

station	Papeete		Rikitea		Tubuai		Rangiroa
	ΔRSLy (mm/year)	Δ*h* (mm/year)	ΔRSLy (mm/year)	Δ*h* (mm/year)	ΔRSLy (mm/year)	Δ*h* (mm/year)	ΔRSLy (mm/year)
Becker et al., 2012 [3]	34 years	11.4years	40 years		2009–2013	2009–2013	2009–2014
	2.9 ± 0.5	−0.4 ± 0.1	2.1 ± 0.4		−9.4 ± 15.1	−0.5 ± 0.5	9.1 ± 6.0
Martinez et al., 2019 [4]	1969–2014	2004–2013	1968–2015	2000–2016			
	3.2 ± 0.4	−1.9 ± 0.2	1.7 ± 0.3	−1.0 ± 0.4			
Fadil et al., 2011 [21]		1998–2009					
		−0.5 ± 0.1					

ΔRSLy: annual relative sea level trend, Δh: vertical motion rate from GPS observations.

6. Conclusions

This work provides cleaned, calibrated hourly seal-level data, with a verified time-tagging, for the five tide gauge geodetic stations installed in French Polynesia by UPF and maintained by SHOM for 2008–2020. This data set can be accessed at NCEI [1]. In Mangareva, the UPF station results are also compared with the University of Hawaii station (RikiteaUH).

The tidal pattern is purely semi-diurnal with a large annual modulation of M2 amplitude. The amplitude and the phase of the main semi-diurnal waves M2 and S2 is in agreement with the values predicted by the ocean tides model FES04, except in Rangiroa and Makemo, where the lagoon is damping the tidal signal. The annual meteorological wave is generally close to 3 cm but reaches 7 cm in Makemo, where large sea swell events produce sea level rise up to 7.5 cm. Although the signal-to-noise ratio is low, it is possible to extract tiny waves at the submillimetric level, e.g. 3MK2 and 3MO2 as well as the harmonics of M2 and S2, up to degree 11. The nodal waves extracted at RikiteaUH are perfectly coherent with the corresponding principal waves and do not require specific treatment in the tidal prediction model.

We, therefore, reached the first goal of our work: the constitution of a reliable tidal prediction model, including long period waves up to the annual component. It is now possible to get reliable non-tidal variations of the sea level at centimeter level.

The determination of the sea-level variations with respect to the grounded tide gauge benchmark (RSL) is still challenging, due to the remaining fluctuations of instrumental or geophysical (mainly meteorological) origin. Moreover, a time interval of 13 years is too short to obtain reliable results. It was possible to determine tentatively variations of the RSL in all the stations except Makemo and Mangareva, where the internal error is too large. In Vairao and RikiteaUH, there is a good agreement with previous investigations concerning the relative sea-level annual rate of change (ΔRSLy). Results at Tubuai and Rangiroa should be further investigated as anomalous results were already reported [4].

The final goal must include the modeling of the remaining fluctuations, and the establishment of a common datum for the five tide gauges with respect to a reference ellipsoid, through GNSS positioning [21], in order to observe true mean sea-level changes.

Declaration of competing interest

The authors declare that they have no known competing financial interests or personal relationships that could have appeared to influence the work reported in this paper.

Acknowledgements

We thank all the successive Chief Officers of the local outposts of SHOM in French Polynesia for their dedication in the maintenance of the network of the tide gauges, and we are grateful to the anonymous reviewer who enriched the bibliography concerning the sea level variations in tropical Pacific islands. We thank Dr. Benoit Stoll, from the geomatics department of UPF, for Fig. 1.

Pr. Jean-Pierre Barriot acknowledges many sources of funding over the years from several institutions belonging to the central government of France (CNRS, CNES, ANR, SHOM, Ministère de l'Outre-Mer, FondsPacifique) and the local authorities of French Polynesia (UPF, Haut-Commissariat de la République, local government of French Polynesia).Dr. Fangzhao Zhang acknowledges funding from the “Talent Introduction Scientific Research Start-Up Fund” of Shandong University of Science and Technology (Grant number 0104060510217), and the “Open Fund of State Key Laboratory of Geodesy and Earth's Dynamics” (Grant number SKLGED2021-3-5).

References

[1] J.-P. Barriot, Fangzhao Zhang, B. Ducarme, G. Woppelmann, G. André, A. Gabillon, SEA LEVEL collected from TIDE STATIONS in South Pacific Ocean from 2009-06-13 to 2021-01-28 (NCEI accession 0244182). NOAA National Centers for Environmental Information. https://www.ncei.noaa.gov/archive/accession/0244182.

[2] A. Cazenave, H. Palanisamy, M. Ablain, Contemporary sea level changes from satellite altimetry: what have we learned? What are the new challenges? Adv. Space Res. 627 (2018) 1639–1653, https://doi.org/10.1016/j.asr.2018.07.017. ISSN 0273-1177, https://www.sciencedirect.com/science/article/pii/S0273117718305799.

[3] M. Becker, B. Meyssignac, C. Letetrel, W. Llovel, A. Cazenave, T. Delcroix, Sea level variations at tropical Pacific islands since 1950, Global Planetary Changes 80–81 (2012) 85–98.

[4] A. Martinez-Asensio, G. Wöppelmann, V. Ballu, M. Becker, L. Testut, A.K. Magnan, V.K.E. Duvat, 2019. Relative sea-level rise and the influence of vertical land motion at Tropical Pacific Islands, Global Planet. Change 176 (2019) 132–143. https://www.sciencedirect.com/science/article/pii/S0921818118306751.

[5] G. Wöppelmann, M. Marcos, Vertical land motion as a key to understanding sea level change and variability, Rev. Geophys. 54 (1) (2016) 64–92, https://doi.org/10.1002/2015RG000502.

[6] MCO des marégraphes côtiers numériques(MCN) du Pacifique. https://agora.shom.fr/docQual/2021/GU/GU2021%96007.

[7] Flanders Marine Institute (VLIZ); Intergovernmental Oceanographic Commission (Ioc), Sea level station monitoring facility. http://www.ioc-sealevelmonitoring.org.

[8] J.-P. Barriot, J. Serafini, L. Sichoix, D. Reymond, O. Hyvernaud, The tsunami of March 11, 2011 as observed by the network of tide gauges of French Polynesia, J. Mar. Sci. Technol. 20 (6) (2012) 639–646, https://doi.org/10.6119/JMST-012-0430-1.

[9] J.-P. Barriot, Fangzhao Zhang, B. Ducarme, G. Woppelmann, G. André, A. Gabillon. A database for sea level monitoring in French Polynesia. Accepted for publication in Geosciences Data Journal.

[10] M. Van Camp, P. Vauterin, Tsoft: graphical and interactive software for the analysis of time series and Earth tides, Comput. Geosci. 31 (2005) 631–640, https://doi.org/10.1016/j.cageo.2004.11.015.

[11] H.G. Wenzel, Format and structure for the exchange of high precision tidal data, Bull.Inf. Marées Terrestres 121 (1995) 9097–9101. http://www.bim-icet.org/.

[12] B. Ducarme, K. Schueller, Canonical wave grouping as the key to optimal tidal analysis, Bull. Inf. Marées Terrestres 150 (2018) 12131–12245. http://www.bim-icet.org/.

[13] K. Schueller, Theoretical basis for Earth Tide analysis with the new ETERNA34-ANA-V4.0 program, Bull.Inf. Marées Terrestres 149 (2015) 12024–12061. http://www.bim-icet.org/.

[14] K. Schueller, Theoretical basis for Earth tide analysis and prediction, Documentation ET34- X-Vmn. http://ggp.bkg.bund.de/eterna/.

[15] TSoft Manual, version 2.2.10. http://seismologie.be/en/downloads/tsoft.

[16] H.G. Wenzel, The nanogal software: Earth tide data processing package ETERNA 3.30, Bull.Inf. Marées Terrestres 124 (1996) 9425–9439. http://www.bim-icet.org/.

[17] J.P. van der Stok, Wind and water, currents, tides and tidal streams in the East Indian Archipelago, Batavia (1897).

[18] A. Courtier, Marées, Service Hydrographique de la Marine, 1938. Paris, https://journals.lib.unb.ca/index.php/ihr/article/download/27428/1882520184.

[19] F. Lyard, F. Lefevre, T.H. Letellier, O. Francis, 2006. Modelling the global ocean tides: modern insights from FES2004, Ocean Dynam. 56 (2006) 394–415.

[20] R.D. Ray, First global observations of third-degree ocean tides, Sci. Adv. 6 48 (2020) eabd4744, https://doi.org/10.1126/sciadv.abd4744.

[21] A. Fadil, L. Sichoix, J.-P. Barriot, P. Ortéga, P. Willis, Evidence for a slow subsidence of the Tahiti Island from GPS, DORIS, and combined satellite altimetry and tide gauge sea level records. C. R, Geoscience 343 (5) (2011) 331–341, https://doi.org/10.1016/j.crte.2011.02.002.

[22] Gsfc, Global mean sea level trend from integrated Multi-Mission ocean altimeters TOPEX/Poseidon, Jason-1, OSTM/Jason-2, and Jason-3, 2021, https://doi.org/10.5067/GMSLM-TJ151. Version 5.1. Ver. 5.1 PO.DAAC, CA, USA.

Bernard Ducarme got his Ph.D. degree in Physics in 1973. He worked for 40 years at the Royal Observatory of Belgium in gravimetry and Earth tides. He was Director of the International Centre for Earth Tides between 1999 and 2008. He is an Emeritus Professor at the Catholic University of Louvain.